Optimizing the Target-based Calibration Procedure of Terrestrial Laser Scanners

Optimierung des zielzeichenbasierten Kalibrierprozesses terrestrischer Laserscanner

Tomislav Medić, Christoph Holst, Heiner Kuhlmann

Terrestrial laser scanner (TLS) measurements suffer from systematic errors due to internal misalignments. The magnitude of the resulting errors in the point cloud exceeds the magnitude of random errors in many applications. Hence, the task of calibration is important for using laser scanners at accuracy demanding applications. However, user-oriented calibration methods are still an active research subject. The majority of the work on this topic relies on the self-calibration of terrestrial laser scanners using targets. The existing solutions could benefit from further optimization, which would lead to a more efficient and user-friendly calibration process. This work aims at improving existing strategies for the target-based TLS calibration by improving the functional and stochastic model for TLS calibration, as well as conducting a sensitivity analysis to support the calibration field design. Based on the latter results, we implement a permanent calibration facility at the University of Bonn. The latter is used to calibrate a Leica ScanStation P20 terrestrial laser scanner. The success of the calibration is empirically demonstrated by reduced measurement errors at a typical TLS measurement example.

Keywords: TLS, laser scanning, self-calibration, accuracy, point clouds

Messungen terrestrischer Laserscanner (TLS) weisen systematische Abweichungen aufgrund interner Ausrichtungsabweichungen auf. Die Größe der resultierenden Abweichungen in der Punktwolke übersteigt in vielen Anwendungen die Größe zufälliger Abweichungen. Um Laserscanner für Anwendungen mit hohen Genauigkeitsanforderungen einsetzen zu können, ist daher eine Kalibrierung des Instruments unerlässlich. Kalibrierprozesse, die der Nutzer selber durchführen kann, sind nach wie vor ein aktuelles Forschungsthema. Der Großteil der Arbeit zu diesem Thema beruht auf der Selbstkalibrierung von terrestrischen Laserscannern unter Verwendung von Zielzeichen. Vorhandene Lösungen sind oftmals wenig effizient und/oder wenig benutzerfreundlich; Optimierungen sind hier sinnvoll. Diese Arbeit zielt darauf ab, bestehende Strategien für die zielbasierte TLS-Kalibrierung durch Anpassungen im funktionalen und stochastischen Modell zu verbessern und eine Sensitivitätsanalyse zum Design des Kalibrierfelds durchzuführen. Basierend auf den letztgenannten Ergebnissen installieren wir ein permanentes Kalibrierfeld in einer Einrichtung der Universität Bonn. Für die Leica ScanStation P20 belegen wir den Erfolg der Kalibrierung empirisch durch reduzierte Messabweichungen bei einem typischen TLS-Messbeispiel.

Schlüsselwörter: TLS, Laserscanning, Selbstkalibrierung, Genauigkeit, Punktwolken

1 INTRODUCTION

The terrestrial laser scanner (TLS) is a standard instrument in the toolbox of geodetic engineers. It rapidly acquires accurate 3D data about its environment through highly dense pointwise measurements over the wide field of view. The product is a point cloud, which is often colored according to the intensity of the reflected laser beam. TLSs are used for a variety of applications, such as cultural heritage documentation, engineering, as-built modeling, forensics, etc. /Vosselman & Maas 2010/. Only a small subset of these applications has high demands towards measurement accuracy. The typical examples are deformation monitoring /Mukupa et al. 2017/ and reverse engineering /Fagan et al. 2018/.

To achieve the required measurement accuracy, manufacturers put a tremendous effort into the production and assembly of all instrument components. However, these processes are not flawless and the off-the-shelf instruments are not geometrically perfect. Additionally, the internal geometry can change over time due to long-term utilization, suffered stresses and extreme atmospheric conditions. The resulting mechanical misalignments cause systematic displacements (errors) of the measured points reducing the accuracy of the point cloud /Heinz et al. 2018/. These misalignments need to be modeled mathematically. To overcome this issue, manufacturers use comprehensive factory calibrations after the instrument assembly, and they advise repeated calibration in regular time intervals (typically 1 or 2 years) /Walsh 2015/. However, there are still several problems concerning some of the end-users.

Firstly, the calibration process is generally treated as a company secret. Therefore, we do not know exact misalignments being calibrated, their accuracy or stability over time. The only certainty is that if we follow the manufacturer's instructions, the instruments will work according to specifications /Holst et al. 2018a/ – sufficient for most users. Secondly, advised repeated calibration is a burdening event for typical geodetic offices because it usually requires several weeks and it can cost several thousands of euros (personal correspondence with the manufacturers). There are certain alternatives, but they lack in comprehensiveness and reliability. For example, some manufacturers like Leica Geosystems and FARO Inc. provide user calibration approaches, which can reduce systematic errors in the measurements to some extent (e. g. Leica's "Check and Adjust" and Faro's "On-site compensation"). However, those approaches do not provide detailed information about estimated calibration parameters accounting for mechanical misalignments, their accuracy, and their influence on the point cloud.

As it is not possible to force the manufacturers to share their company secrets, the main thing missing is a user-oriented calibration approach similar to the existing ones for total stations. The main objective of this article is to describe the efforts of the Institute of Geodesy and Geoinformation at the University of Bonn to reach the latter aim. Therefore, the following sections describe the steps made in the scope of developing a generally accepted, user-oriented calibration approach.

2 STATE-OF-THE-ART

In the last decade, multiple articles were published aiming at developing and improving user-oriented calibration approaches. Hence, today, there are several approaches using different objects for the calibration, such as cylinders /Chan et al. 2015/, spheres /Neitzel 2006/, planes /Chow et al. 2013/, paraboloids /Holst & Kuhlmann 2014/, targets /Lichti 2007/ or keypoints /Medić et al. 2019a/. Most of them are considered self-calibration approaches because all calibration parameters are determined simultaneously and without a need of a special calibration facility. All these approaches generally work, and they can successfully reduce the systematic influence of TLS misalignments to a certain degree. However, none of them so far was generally accepted as a user-calibration approach and there are several reasons for that.

Firstly, all mentioned calibration approaches provide parameters which are valid on-site (in-situ), in that very moment, for the very object under investigation. None of the studies questioned the stability of the parameters and the possibility to use them afterward. Secondly, all approaches relying on modeling geometric primitives are realized as best-fit algorithms that use highly correlated TLS measurements. These correlations are disregarded (without exception) due to the lack of sufficient knowledge /Jurek et al. 2017/. This leads to unrealistic estimates of the standard deviation of the estimated calibration parameters. Therefore, they lack objective criteria telling how successful the calibration was. Thirdly, it is hard to guarantee that the geometry found on a certain job will provide a sufficient measurement configuration for revealing and estimating all relevant mechanical misalignments. Additionally, in the case that configuration is not sufficient, it is hard to manipulate planar walls and cylindrical pipes to achieve good measurement configuration. Lastly, most of these methods require long measuring and processing time and they are hard to recreate.

Therefore, the generally accepted user-oriented calibration approach should have the following characteristics. It should be:

- user-friendly and cost-effective – i. e. easily reproducible by qualified engineers,
- comprehensive – i. e. sensitive to detect and model all relevant systematic errors,
- informative – providing all necessary data (standard deviations, correlations) and
- it needs to provide a mechanically explainable set of the calibration parameters.

The most promising candidate for fulfilling all given criteria is the target-based self-calibration approach /Lichti 2007/. Therefore, from all previously mentioned approaches, we decided to pursue our goal through the optimization of the target based self-calibration. The principle of this approach, as well as the steps in optimizing it, is described in the following sections.

3 TLS CONSTRUCTION

TLSs can be separated into three categories according to their field-of-view and underlying mechanism on camera, hybrid and panoramic TLSs /Vosselman & Maas 2010/. Due to different mechanisms, the

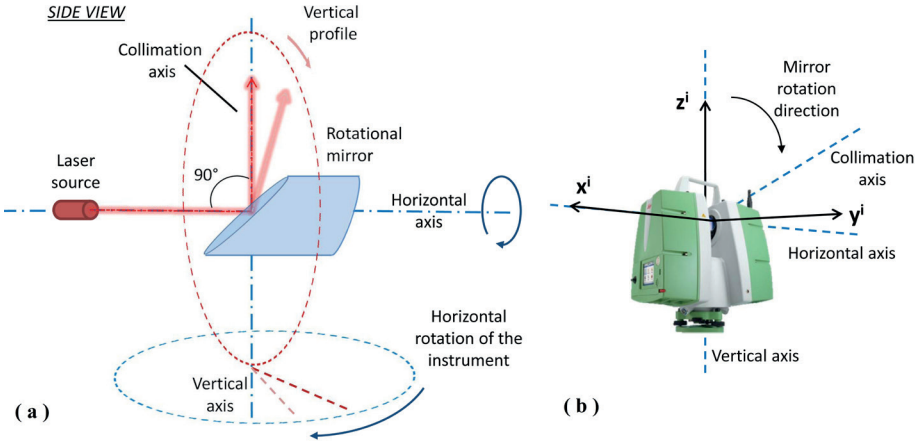

Fig. 1 | (a) Perfect panoramic TLS geometry, (b) Local Cartesian coordinate system of the scanner with a respect to the main instrument axes /Medić et al. 2017/

optimization of the calibration approach for each of them is different. Hence, this work focuses only on panoramic TLSs, as they are the most often used type in engineering geodesy.

Panoramic TLSs are capable of measuring the whole 3D volume around them, except a small conical area beneath the instrument. They are similar to total stations. They have three main axes which are supposed to be orthogonal in the perfect case and the main sensors are horizontal and vertical angular encoders and EDM unit (rangefinder). However, TLSs are more complex due to the rotating mirror used to deflect the laser beam. *Fig. 1a* represents the perfect geometry of TLSs, which is never achieved in practice. The rangefinder fires the laser beam on the rotating mirror, which is inclined for 45°. The laser beam reflects outside the instrument to the measured point, forming a right angle. The mirror rotates around the horizontal axis and that way vertical profiles are measured. Additionally, the whole instrument is rotating around the vertical axis. These polar measurements (ranges, horizontal and vertical angles) are automatically recalculated to Cartesian coordinates of the local scanner coordinate system with the origin in the middle of the rotating mirror (*Fig. 1b*) and stored in the instrument.

An important characteristic of the panoramic TLSs is that their mechanism allows them to use two-face measurements similar to the total station. Namely, only after half of the rotation around the vertical axis, the whole 3D environment is captured in a way that part of the environment is measured from the front side of the scanner, and part from the back side. If the instrument's rotation continues to finish the full circle around the vertical axis, the same scenery will be measured again. However, this time, the parts of the environment measured from the front and the back will be swapped. This measurement principle can reveal multiple systematic errors and it is commonly used in the geodetic community for the calibration of total stations /Schofield & Breach 2007/.

Several possible mechanical misalignments can cause systematic errors in TLS measurements and there are two ways to divide them. First, they can be divided into tilts (rotations) and offsets (translations) of the main instrument components. The tilts have a higher impact on measurement quality because the magnitude of the related systematic errors grows with the distance. On the contrary, the systematic errors of the offsets are constant concerning the distance and usually small in magnitude. Second way to divide the TLS misalignments is by the instrument part which is tilted or offset on laser source tilts and offsets (*Fig. 2a* and *Fig. 2b*), mirror tilts and offsets (*Fig. 2c* and *Fig. 2d*) and horizontal axis tilt and offset (*Fig. 2e* and *Fig. 2f*). The remaining systematic errors are equal to the total station errors and those are rangefinder errors, vertical index offset, and angular encoder errors. The list of all relevant systematic errors (calibration parameters) for TLSs is given in *Table 1*. The parameter nomenclature (symbols) is adopted from the American National Institute of Standards and Technology and the readers are referred to /Muralikrishnan et al. 2015a/ for more details. The list gives an overview of which of the TLS parameters also exist in the same or similar form in total stations, which parameters can be revealed using two-face measurements and which parameters exist in the high-end TLSs. By high-end, we denote instruments

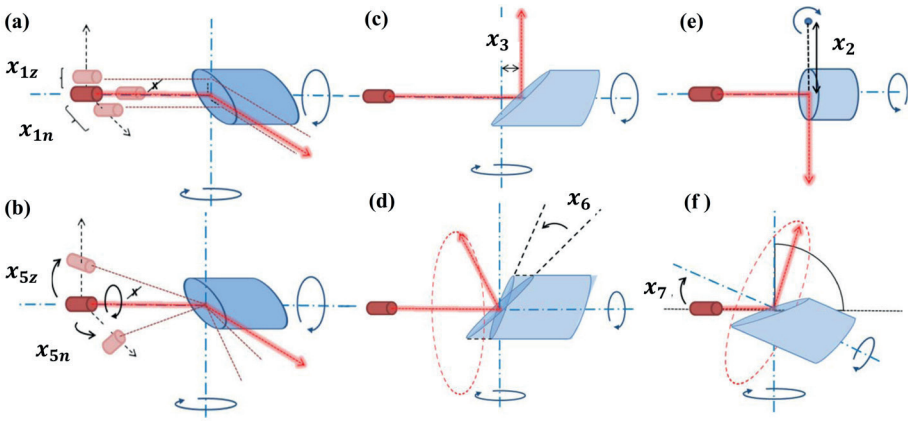

Fig. 2 | Mechanical misalignments of panoramic TLSs; (a), (b) laser offsets & tilts; (c), (d) mirror offset & tilt; (e), (f) horizontal axis offset & tilt /Medic´ et al. 2017/

Description	Parameter	TS	2-faces	high-end
Horizontal beam offset	x_{1n}	similar	no	yes
Vertical beam offset	x_{1z}	no	yes	yes
Horizontal axis offset	x_2	similar	yes	yes
Mirror offset	x_3	no	yes	yes
Vertical index offset	x_4	yes	yes	yes
Horizontal beam tilt	x_{5n}	similar	yes	yes
Vertical beam tilt	x_{5z}	similar	no	yes
Mirror tilt	x_6	similar	yes	yes
Horizontal axis error (tilt)	x_7	yes	yes	yes
Horizontal angle encoder eccentricity	x_{8x}	yes	yes	no
Horizontal angle encoder eccentricity	x_{8y}	yes	yes	no
Vertical angle encoder eccentricity	x_{9n}	yes	yes	no
Vertical angle encoder eccentricity	x_{9z}	yes	no	no
Second order scale error in the horizontal angle encoder	x_{11a}	yes	no	no
Second order scale error in the horizontal angle encoder	x_{11b}	yes	no	no
Second order scale error in the vertical angle encoder	x_{12a}	yes	yes	no
Second order scale error in the vertical angle encoder	x_{12b}	yes	no	no
Rangefinder offset	x_{10}	yes	no	yes
Rangefinder scale error	/	yes	no	yes
Rangefinder cyclic error	/	yes	no	yes*

* existing only in TLSs using phase-shift distance measuring principle

Tab. 1 | The comprehensive list of mechanical misalignments in TLS: nomenclature by NIST, existence in total stations, two-face sensitivity, and existence in high-end TLSs

having high-quality components including angular encoders with multiple reading heads, which eliminates a considerable amount of overall possible TLS misalignments /Walsh 2015/. The rangefinder related systematic errors, such as scale and cyclic error, are still best estimated through established laboratory procedures using comparator track /Schofield & Breach 2007/. Therefore, they are usually excluded from the self-calibration approaches.

4 TARGET-BASED SELF-CALIBRATION

4.1 Concept

The target-based self-calibration requires that targets are distributed in the environment and scanned from several stations. Afterward, the point cloud parts belonging to the targets are extracted and transformed into the image representation of EDM intensity measurements. Finally, using different detection algorithms, the target centers are accurately estimated /Janßen et al. 2019/. These target centers are later transformed from 2D image coordinates to 3D polar coordinates mimicking the raw instrument measurements. They are treated as observations in the calibration algorithm and they are used to estimate the unknown parameters. The algorithm is realized as the least squares adjustment and it is based on the functional model of rigid body motion, bundle adjustment or a scanner registration:

$$\boldsymbol{f}_j^i = \boldsymbol{R}^i_{(k,\phi,\omega)}\boldsymbol{xyz}_j^i + \boldsymbol{T}^i_{(X,Y,Z)} - \boldsymbol{XYZ}_j^{ref.} = \boldsymbol{0}, \tag{1}$$

where $i = 1, 2, \ldots, s$; $j = 1, 2, \ldots, p$; s and p are total numbers of scanner stations and targets used in the experiment. The estimated parameters are separated in the rotation matrix $\boldsymbol{R}^i_{(k,\phi,\omega)}$ defined with Euler angles (k, ϕ, ω), the translation vector $\boldsymbol{T}^i_{(X,Y,Z)}$ and the vector of the target coordinates in the reference system $\boldsymbol{XYZ}_j^{ref.}$. The measurement vector from the scanner station i to the target j in the local coordinate system is equal to

$$\boldsymbol{xyz}_j^i = \begin{bmatrix} x_j^i \\ y_j^i \\ z_j^i \end{bmatrix} = \begin{bmatrix} \left(r_j^i + \Delta r_j^i\right)\sin\left(\theta_j^i + \Delta\theta_j^i\right)\sin\left(\varphi_j^i + \Delta\varphi_j^i\right) \\ \left(r_j^i + \Delta r_j^i\right)\sin\left(\theta_j^i + \Delta\theta_j^i\right)\cos\left(\varphi_j^i + \Delta\varphi_j^i\right) \\ \left(r_j^i + \Delta r_j^i\right)\cos\left(\theta_j^i + \Delta\theta_j^i\right) \end{bmatrix}, \tag{2}$$

where x_j^i, y_j^i, z_j^i, are Cartesian coordinates of the target which are transformed to the polar coordinates $r_j^i, \varphi_j^i, \theta_j^i$ – range, horizontal and vertical angle measurements, while $\Delta r_j^i, \Delta\varphi_j^i, \Delta\theta_j^i$ are registration errors. The only difference between the usual point cloud registration and the TLS calibration is that the registration errors are now decomposed on the random measurement noise and the systematic errors due to TLS misalignments.

4.2 Why targets?

There are several reasons why the target-based approach is the most promising candidate to become a generally accepted user-oriented calibration approach. First, instead of using relatively noisy raw single point measurements, this approach uses target centers. The target centers are derived from hundreds or thousands of

measurements and, therefore, they are much more precise /Janßen et al. 2018/. Second, with this approach, we are moving from nearly continuous (areal) measurements to single point measurements. This means that instead of using highly dense and highly correlated raw TLS observations, we use sparse pointwise observations. That brings two important advantages. One is that we can justify disregarding these high unknown correlations. The other one is that we can use statistical tools that have been developing for decades for pointwise measurements of instruments such as total stations or GNSS receivers. Third, this means that from a very general task of improving scanner calibration the aim is changed to the task of optimization of geodetic networks. Again, something that is well studied in the past. Additionally, it is easy to manipulate the position of targets (measurement geometry) in the way that we can achieve sensitivity to estimate all relevant calibration parameters. Finally, targets are inexpensive and easy to handle.

4.3 Current standpoint

The target-based self-calibration was successfully used by multiple authors so far, e. g. /Lichti 2007/, /Reshetyuk 2010/, /Abbas et al. 2014/. Typical characteristics of the documented calibration experiments are:

- they use numerous targets (60 – 300),
- multiple scans from multiple stations (4 – 16),
- they are usually conducted in small rooms, and
- they mainly rely on heavy redundancy.

Chow et al. (2013) presented a typical measurement configuration with 120 targets measured with 6 scans from two scanner stations in a room with dimensions of 14 × 11 × 3m. This results in long calibration field assembly, measurement, and processing times and makes the whole process less efficient. Therefore, this calibration approach would benefit from further optimization. Several issues need to be tackled to realize this optimization. Namely, it is necessary to define the correct functional model of the calibration parameters. Further, it is required to define the correct stochastic model describing the true measurement uncertainty in a calibration field. Finally, it is necessary to investigate which relative positions of targets and scanner stations are sensitive enough to allow revealing and modeling mechanical misalignments. Only after all latter goals are realized, the optimization approach will lead to meaningful results. From this point on, our experiments focus on the calibration of the Leica ScanStation P20, but they are transferable to panoramic scanners in general.

5 OPTIMIZING THE CALIBRATION PROCESS

5.1 Functional model

The publications mentioned in the previous section used multiple different mathematical (functional) models to describe TLS mechanical misalignments. Hence, no model could be considered as universally accepted. These functional models are most often based on the known systematic errors of total stations, due to the high similarity of the instruments. The total station models can be separated on a simple model /Abbas et al. 2014/, which consist of only 4 main parameters (trunnion and collimation axis error, vertical index and rangefinder offset), and more comprehensive models /Lichti 2007/. Some studies extended the list of the calibration parameters empirically through observing the behavior of the residuals after the adjustment /Chow et al. 2013/. Additionally, some publications used functional models based on panoramic cameras /Parian & Gruen 2010/. As previously stated, using any of these models leads to calibration parameters, which are valid only on-site. For achieving the parameter stability and their reusability it is necessary to define parameters with clear mechanical interpretation, as it will be demonstrated in the following sections.

Only recently researches at the American National Institute of Standards and Technology derived a functional model which describes systematic errors based on the true geometry of panoramic TLSs /Muralikrishnan et al. 2015a/. It consists of 18 parameters that describe different tilts and offsets of the main TLS components as well as the systematic errors of the angular encoders (*Tab. 1*). This functional model was tested in a big run-off experiment and generally accepted from the majority of the leading TLS manufacturers /Muralikrishnan et al. 2016/. It is worth noting that the latter model is developed for a series of consecutive test procedures that are realized in controlled laboratory conditions with reference laser tracker measurements. Hence, some modification steps are necessary to use this functional model in the target-based self-calibration.

We investigated this functional model and made necessary adaptations. Some parameters need to be combined (x_{5z} and x_7, x_{1zn}, and x_2). Due to the identical systematic impact on measurements, hence, the same functional model, they cannot be estimated separately without a bias. Additionally, some parameters were removed due to advancements in the measurement technology. Namely, new angular encoders in the high-end TLSs use four reading heads to provide each angular measurement. This leads to averaging out and elimination of multiple systematic errors (*Tab. 1*). Therefore, the final functional model of calibration parameters for high-end panoramic TLSs in a target-based self-calibration is defined as:

$$\Delta r_j^i = x_2 \sin\left(\theta_j^i\right) + x_{10} + v_{r_j^i}, \tag{3}$$

$$\Delta \varphi_j^i = \frac{x_{1z}}{r_j^i \tan\left(\theta_j^i\right)} + \frac{x_3}{r_j^i \sin\left(\theta_j^i\right)} + \frac{x_{5z-7}}{\tan\left(\theta_j^i\right)} + \frac{2x_6}{\sin\left(\theta_j^i\right)} + \frac{2x_6}{\sin\left(\theta_j^i\right)} + \frac{x_{1n}}{r_j^i} + v_{\varphi_j^i}, \tag{4}$$

$$\Delta \theta_j^i = \frac{x_{1n+1}\cos\left(\theta_j^i\right)}{r_j^i} + x_4 + x_{5n}\cos\left(\theta_j^i\right) - \frac{x_{1z}\sin\left(\theta_j^i\right)}{r_j^i} - x_{5z}\sin\left(\theta_j^i\right) + v_{\theta_j^i}, \tag{5}$$

where $v_{r_j^i}$, $v_{\varphi_j^i}$, $v_{\theta_j^i}$ are the adjustment residuals describing the random measurement errors.

Additionally, we explicitly implemented two-face measurements in target-based self-calibration through modification of the usual equations used to recalculate point cloud Cartesian coordinates into the polar coordinates. This part of the functional model did not

receive sufficient attention in most of the related publications. There are several different ways angles are parameterized in the literature /Lichti 2007/, /Muralikrishnan et al. 2015a/. We decided to represent the angular motion, both in the horizontal and vertical angles, with the values from 0° to 360° (typically used in total stations), which makes it easy to use two-face measurements in the conjunction with the latter functional model of calibration parameters. We use the following functions:

$$r_j^i = \sqrt{x_j^{i^2} + y_j^{i^2} + z_j^{i^2}},\ \varphi_j^i = \arctan\left(\frac{x_j^i}{y_j^i}\right),\ \theta_j^i = \arccos\left(\frac{z_j^i}{r_j^i}\right). \quad (6)$$

In the first scan of two-face measurements, the value of 180° is added to the horizontal angles if the calculated angle is negative. This is the case because the scanner made only half of the rotation around the vertical axis, using the same horizontal angle readings for points measured both in the front and in the back. In the second scan of two-face measurements, the scanner uses a new set of diagonally opposite angular readings for the horizontal angles. Therefore, in the second scan, the value of 180° is added if the calculated angle is positive and 360° if the angle is negative. The position of the mirror (front and back side) is easily tracked with the x_j^i coordinate value. If this coordinate in the first scan is negative, the calculated vertical angle is subtracted from 360°. In the second scan, the case is the opposite. If the x_j^i coordinate is positive the calculated vertical angle is subtracted from 360°.

The described calculation of polar coordinates is valid for Leica ScanStation P20. Special care should be placed in defining the local scanner coordinate system correctly. Namely, the latter scanner uses the *y-headed* right-handed clockwise-rotating coordinate system. That means that the 0° direction of horizontal angles is in the direction of $+y^i$ axis and 180° at $-y^i$ (*Fig. 1*). If the same functional model is used for e. g. Leica BLK360, the calibration will fail. Namely, the latter scanner is *x-headed*. Hence, the 0° direction coincides with $+x^i$ and 180° with $-x^i$ direction. This is a banal point, but often unconsidered. Not considering this leads to wrong conclusions which parts of the environment are measured in the front and which in the back of the scanner.

In the experiment described in /Medić et al. 2017/, we successfully estimated the derived set of calibration parameters (Eqs. (*3*) –(*5*)) and notably improved the measurement quality. Additionally, we proved that most of the parameters (8 out of 11) can be directly estimated using only two-face measurements from a single scanner station. Therefore, we achieved the first prerequisite for the optimization of the calibration – an accurate functional model.

5.2 Stochastic model

Previous publications relied on values provided in the manufacturer's specifications for a single point accuracy to define their stochastic models. This means that they usually used 2–3 scalar values (1 for ranges and 1 or 2 for angles) to describe the measurement uncertainty of all measurements within the calibration adjustment. However, these stochastic models are not accurate because the target-based self-calibration uses target centers and not raw single point measurements. The target centers are derived from multiple measurements, using the image representation of EDM intensity measurements. Hence, they have different uncertainty characteristics, which depend on multiple factors such as measurement resolution, scanner to target distance and angle of incidence. Therefore, the usual stochastic models are overly simplified.

To define a more realistic stochastic model, we empirically investigated the precision of the target center estimation and we compared it with the values that are given in manufacturer's specifications /Medić et al. 2019b/. The empirical precision is simply estimated as a standard deviation of repeatedly estimated target centers. Using this value for the stochastic model for TLS calibration is justified because the precision and the accuracy of the target center should be approximately the same. Namely, there are four sources of systematic influences in TLS measurements that can cause the difference between accuracy and precision. Those are influences of instrumental errors, atmosphere, measurement geometry (distance and angle of incidence) and object properties /Soudarissanane 2016/. In TLS calibration instrumental errors are included in the functional model, and therefore, they do not need to be included in the stochastic model. The influence of the atmosphere can be neglected on typical measurement distances for panoramic TLSs. The object properties are the same for all targets in one calibration experiment. Hence, their systematic influence is the same, it is averaged out and it does not impact the measurement accuracy. Finally, measurement geometry needs to be accounted for. Therefore, in our experiments, we observed the target centers with different measurement configurations.

Figure 3 presents notable differences between the values from manufacturer's specifications (red lines) and the precision of the target centers (black curves) for Leica ScanStation P20 /Leica 2015/, for ranges (top) and horizontal angles (bottom). Not considering these differences can cause bias in the parameter estimates as well as the wrong estimate of the standard deviation of calibration parameters. Additionally, the precision is not constant – it changes with the distance. This is generally expected for the range measurements (although often disregarded) but never considered for the angular measurements. Therefore, the accurate stochastic model cannot be represented by using only 2 or 3 scalar values.

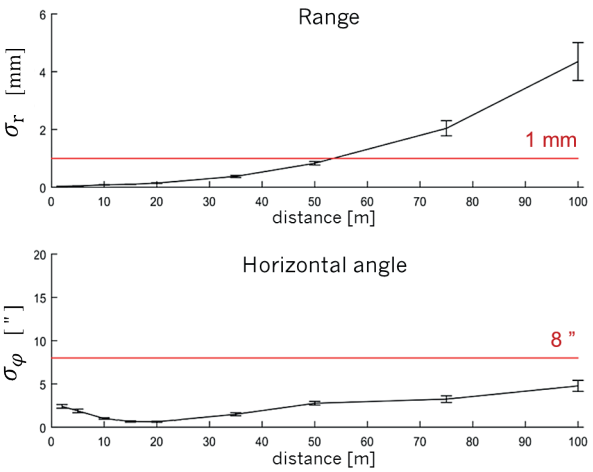

Fig. 3 | Values from the manufacturer's specifications (red) vs. empirical data (black)

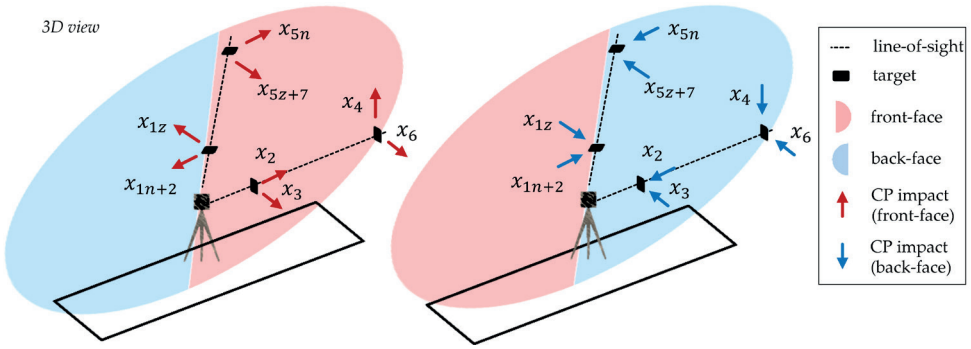

Fig. 4 | Sensitive measurement configurations for estimating the two-face sensitive parameters using two-face differences (CP – calibration parameter)

Although the change for angular measurements seems small, it shows that angular measurements can be four times more precise in some distances than in others. Hence, there is the global minimum in which angular measurements achieve the highest precision. We used this empirical data to form the correct stochastic model in a form of the look-up table and we used it for the optimization of TLS calibration.

5.3 Parameter sensitivity

The third issue in the optimization of TLS calibration is achieving a network geometry which is sufficiently sensitive to estimate all relevant TLS misalignments. /Muralikrishnan et al. 2015b/ conducted such a sensitivity analysis to estimate which point locations are more and which are less sensitive to estimate the misalignments. This study relies on the reference point field realized with laser tracker measurements in the controlled laboratory conditions. Additionally, it does not use two-face measurements, which are very sensitive to reveal some TLS misalignments. Hence, a new sensitivity analysis is necessary for the target-based self-calibration approach.

We conducted a new sensitivity analysis relying only on targets and TLS measurements – including two-face measurements /Medić et. al. 2019c/. This sensitivity analysis is based on the presented knowledge about the accurate functional model of calibration parameters and the accurate stochastic model for the target centers. For parameters that are sensitive to two-face measurements, we found the best target locations with respect to the scanner station (distance, horizontal and vertical angle). *Fig. 4* presents a short overview of all necessary target locations to successfully estimate all relevant two-face sensitive calibration parameters. In short, it is necessary to observe two targets approximately in the instrument's horizon and two targets with the increased elevation angle (optimally close to the local zenith). For unbiased estimates of the offset parameters, two targets should be placed close to the instrument (few meters distance). Additionally, two targets should be placed further away from the instrument to unbiasedly estimate the tilt parameters (global minimum in *Fig. 3*, approximately 20 m for the Leica ScanStation P20).

For the parameters, which are not two-face sensitive, we derived the sensitive length tests (*Fig. 5*). These length tests work on the principle that the length between two targets (black solid line) is observed from two scanner stations. From one station, the length between the targets should be influenced by the parameter under investigation as least as possible, i. e. the measurement configuration is not sensitive on the impact of the parameter. Here, the length under investigation is only rotated or translated in space, but not deformed. Therefore, it should remain close to a true value. From the second station, the length between the targets needs to change (deform) as much as possible – sensitive measurement configuration. The difference between these two lengths, realized with the most and the least sensitive measurement configuration, gives necessary information for estimating the parameters. The simplest example is estimating the rangefinder offset (x_{10}) with the inside-out test (*Fig. 5, top*), which is commonly used in the geodetic community for testing and calibration of total stations. When the instrument is placed aside the length, the length is only translated in space due to the impact of x_{10}. However, when the instrument is placed between the targets, the length is deformed by twice the rangefinder offset. Comparing these two values allows the estimation of the calibration parameter.

As some of the TLSs on the market cannot use two-face measurements, we additionally derived the length tests for two-face sensitive parameters. Hence, *Fig. 6* presents the alternative solution for the measurement configurations presented in *Fig. 4*. The sensitive measurement configurations are rather simple and they do not differ much from the two-face differences. The only modification is that now two targets are necessary. They should be scanned so that

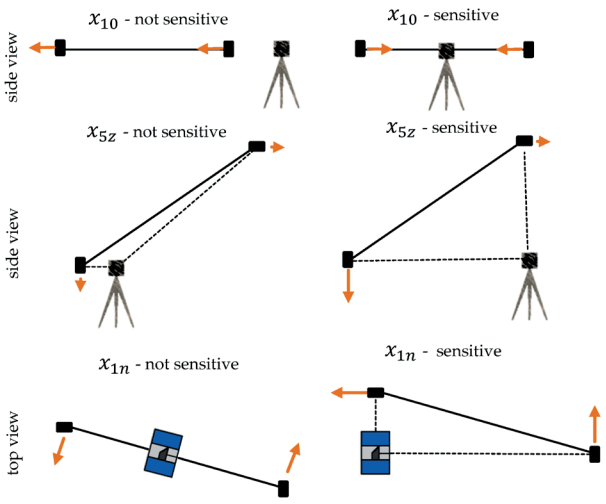

Fig. 5 | Sensitive measurement configuration for estimating the remaining (not two-face sensitive) parameters using the length-tests (orange arrow – magnitude and direction of CP impact).

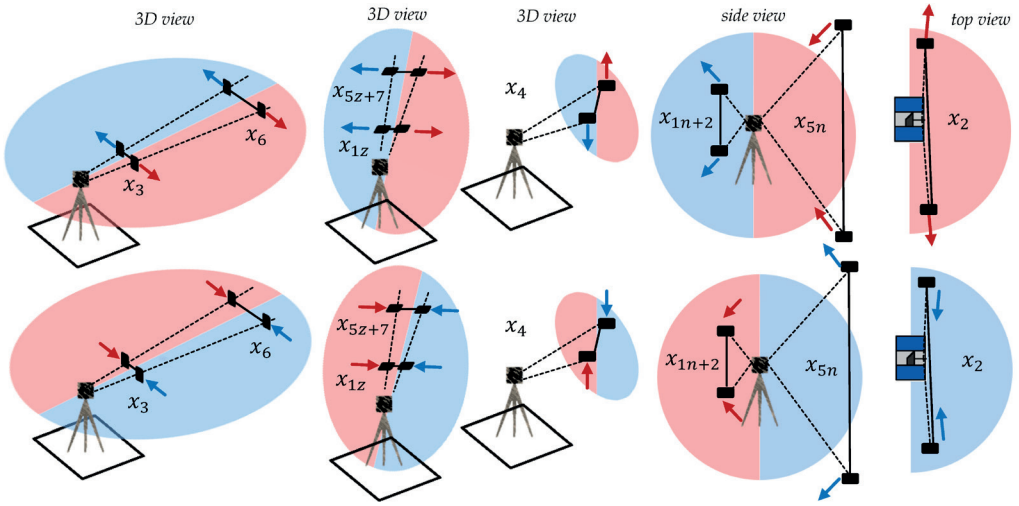

Fig. 6 | Sensitive measurement configurations for estimating the two-face sensitive parameters using the length tests (when the two-face differences are not available)

one target is measured from the front and the other from the back side of the instrument during the same scan for parameters x_3 , x_6, x_{1z}, x_{5z+7}, and x_4. For the rest of the parameters both targets need to be scanned from the same side during one scan. This way the length between the targets will be deformed, e. g. it will be extended, due to the impact of the calibration parameter (*Fig. 6, top*). Now, if the instrument is manually coarsely rotated around the standing axis for approximately 180°, the targets measured in the front and in the back will be swapped. This in turn will cause that the length between the targets is deformed with the same magnitude, but in the opposite direction, e. g. it will be shortened (*Fig. 6, bottom*). The searched calibration parameters equal half of the difference between extended and shortened lengths. For the most sensitive measurement configurations and unbiased parameter estimates, the targets should be placed according to the sketches in *Fig. 6*. Again, for the offset parameters, the test-length should be close to the scanner, while for the tilt parameters, it should be on the distance with the lowest uncertainty of the angular measurements. Hence, the results of this sensitivity analysis provided the last prerequisite for the optimization of the calibration field.

5.6 Calibration field optimization

So far there was only one published attempt of the calibration field optimization /Abbas et al. 2014/ and it was made only for a basic total station model of calibration parameters (Sec. 5.1). Based on the data presented in the previous sections several conclusions can be drawn:

- there are more than 4 relevant calibration parameters that need to be estimated,
- two-face measurements can improve the calibration and reduce the required number of targets,
- measurements at the distances of 15–20 m are necessary to achieve the highest measurement precision, and
- we need a minimum of two stations with carefully placed targets (length tests) to estimate parameters not sensitive to two-face measurements.

In order to achieve the optimized configuration of the calibration field, we conducted a series of simulation experiments. Based on the latter conclusions we tested multiple different positions of TLS stations and target locations by manual trial and error analysis. The best simulation solution is presented in *Figure 7*. In short, we need 14 targets on predefined locations measured from two scanner stations using two-face measurements to accurately estimate all relevant misalignments of high-end panoramic TLSs. We implemented the simulated network in a machine hall with the dimensions

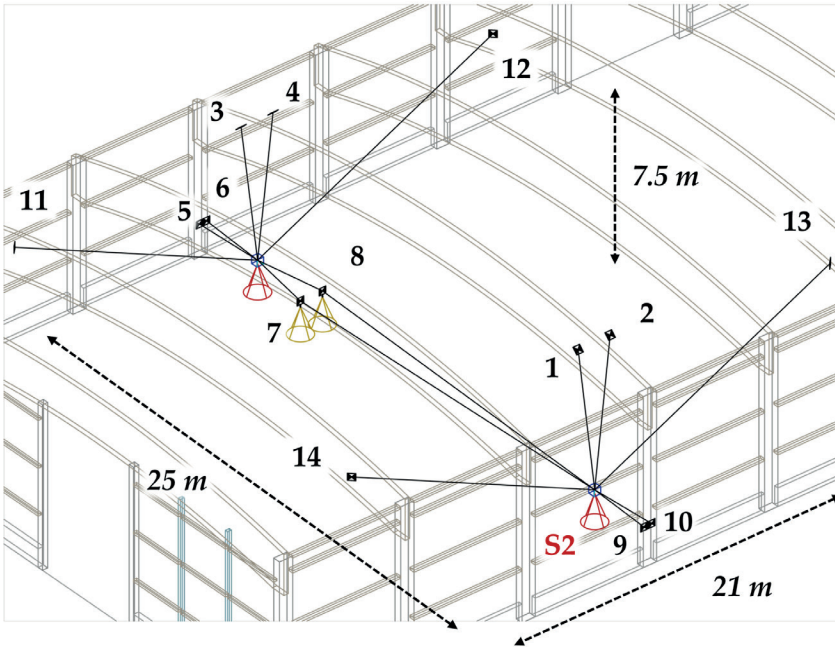

Fig. 7 | Calibration hall /Medić et al. 2020/

of 70×25×9 m (*Fig. 7*) and used it to calibrate the Leica ScanStation P20. The evaluation of the calibration success is presented in the following section.

6 OPTIMIZATION VALIDATION

Using the optimized calibration approach, we notably reduced the residuals of the calibration adjustment (Eq. (*1*)). The realized improvements were comparable or higher in the comparison with the previous publication. This is the usual criteria for the validation of the calibration success. However, it is only proof of the in-situ calibration success.

As we aim at the stable and reusable set of the calibration parameters, we also tested if the estimated parameters can be used for later measurements. We took one typical example of TLS measurements, a wall outside the calibration hall. We measured this wall from one station using two-face measurements and we calculated the differences between the first and the second scan. The differences are computed using the M3C2 algorithm, which is a given plug-in in the CloudCompare open software /Lague et al. 2013/. This way the differences are computed in the direction of the local surface normals. The differences before and after applying the estimated calibration parameters are presented in *Figure 8*. They are colored based on the offset direction (sign). All differences lower than a threshold of 0.5 mm are represented with green color, while all differences breaching the threshold are colored blue and red. In the upper part of the figure, clear systematic trends are recognizable. They abruptly switch signs between the parts measured in the front and parts measured in the back of the scanner. If it would remain unrevealed, such a systematic trend could be mistaken for a deformation in a deformation analysis. These trends are an indication of unmolded instrument misalignments /Holst et al. 2018b/. In the bottom part of the figure, it is visible that applying the calibration parameters removed the latter systematic behavior. The only differences higher than 0.5 mm are showing the random distribution and they are visible on the far left, away from the scanner station. This increased noise is due to high incidence angles and higher distances, which impacts the quality of the reflectorless distance measurements /Soudarissanane 2016/. Hence, this is the definite proof of the successful calibration using the optimized network configuration.

7 CONCLUSION

In the pursuit of our goal, optimizing the target-based self-calibration of TLSs, so far we:

- tackled the issues of defining the accurate functional and stochastic models,
- assured the measurement configuration sensitivity to estimate all relevant calibration parameters,
- defined the optimized design of the calibration field through a series of simulation experiments, and
- implemented and tested the simulated filed design.

The success of the calibration using the proposed improvements was demonstrated on a typical TLS measurement example – the measurement of a building wall. The presented calibration approach is cost-efficient – it requires only 14 inexpensive scanner targets, it takes approximately 1 hour of scanning for Leica ScanStation P20, and processing the data for 14 targets is not time-consuming. Hence, we demonstrated that this calibration approach has the potential to become a generally accepted user-oriented TLS calibration approach.

REFERENCES

Abbas, M. A.; Derek, D. L.; Albert, K. C.; Halim, S.; Zulkepli, M. (2014): An on-Site Approach for the Self-Calibration of Terrestrial Laser Scanner. Measurement 52(2014)1, 111 – 123.

Chan, T. O.; Derek, D. L.; Belton, D. (2015): A Rigorous Cylinder-Based Self-Calibration Approach for Terrestrial Laser Scanners. ISPRS J. Photogramm. Remote Sens. 99, 84 – 99.

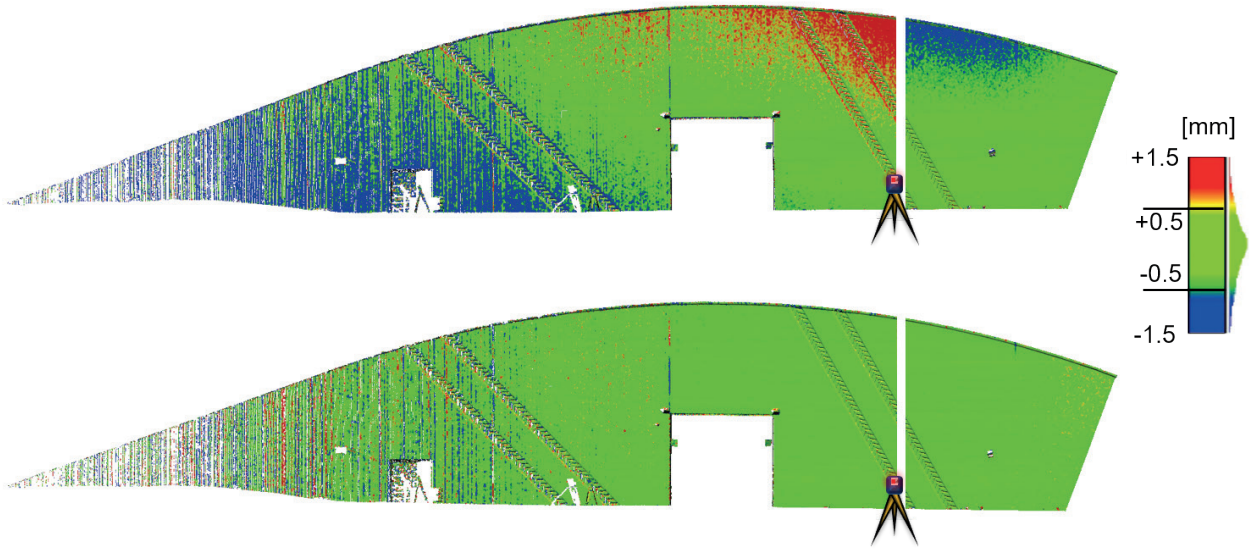

Fig. 8 | Differences between 1st and 2nd scan of two-face measurements, before (top) and after (bottom) applying the calibration parameters (in mm)

Chow, J. C. K.; Derek, D. L.; Glennie, C.; Hartzell, P. (2013): Improvements to and Comparison of Static Terrestrial LiDAR Self-Calibration Methods. Sensors 13(2013)6, 7224–7249.

Fagan, E. M.; De La Torre, O.; Leen, S. B.; Goggins, J. (2018): Validation of the Multi-Objective Structural Optimisation of a Composite Wind Turbine Blade. Composite Structures.

Heinz, E.; Medić, T.; Holst, C.; Kuhlmann, H. (2018): Genauigkeitsbeurteilung von Laserscans anhand realer Messobjekte. In: DVW e.V. (Ed.): Terrestrisches Laserscanning 2018 (TLS 2018). Wißner, Augsburg, DVW-Schriftenreihe 93, 41–56.

Holst, C.; Kuhlmann, H. (2014): Aiming at Self-Calibration of Terrestrial Laser Scanners Using Only One Single Object and One Single Scan. J. Appl. Geodesy 8(2014)4, 295–310.

Holst, C.; Jurek, T.; Blome, M.; Marschel, L.; Petersen, M.; Kersten, T. P.; Mechelke, K.; Lindstaedt, M.; Wehmann, W.; Wunderlich, T.; Wasmeier, P. (2018a): Empirische Ergebnisse von TLS-Prüffeldern: Gibt es Auffälligkeiten? In DVW e.V. (Ed.): Terrestrisches Laserscanning 2018 (TLS 2018). Wißner, Augsburg, DVW-Schriftenreihe 93, 9–40.

Holst, C.; Medić, T.; Kuhlmann, H. (2018b): Dealing with systematic laser scanner errors due to misalignment at area-based deformation analyses. J. Appl. Geodesy 12(2018)2, 169–185.

Janßen, J.; Holst, C.; Kuhlmann, H. (2018): Registrierung mit Targets: Wie genau ist das? In DVW e.V. (Ed.): Terrestrisches Laserscanning 2018 (TLS 2018). Wißner, Augsburg, DVW-Schriftenreihe 93, 75–94.

Janßen, J.; Medić, T.; Kuhlmann, H.; Holst, C. (2019): Decreasing Uncertainty of Target Centre Estimation at Terrestrial Laser Scanning by Choosing Best Algorithm and by Improving Target Design. Remote Sensing 11(2019)7, 845.

Jurek, T.; Kuhlmann, H; Holst, C. (2017): Impact of Spatial Correlations on the Surface Estimation Based on Terrestrial Laser Scanning. J. Appl. Geodesy 11(2017)3, 143–155.

Lague, D.; Brodu, N.; Leroux, L. (2013): Accurate 3D Comparison of Complex Topography with Terrestrial Laser Scanner: Application to the Rangitikei Canyon (N-Z). ISPRS J. Photogramm. Remote Sens. 82, 10–26.

Leica (2015): Leica ScanStation P20 Industry's Best Performing Ultra-High Speed Scanner. Leica Scanstation P20: Datasheet.

Lichti, D. D. (2007): Error Modelling, Calibration and Analysis of an AM-CW Terrestrial Laser Scanner System. ISPRS J. Photogramm. Remote Sens. 61(2007)5, 307–324.

Medić, T.; Holst, C.; Kuhlmann, H. (2017): Towards System Calibration of Panoramic Laser Scanners from a Single Station. Sensors 17(2017)5, 1145.

Medić, T.; Kuhlmann, H.; Holst, C. (2019a): Automatic in-situ self-calibration of a panoramic TLS from a single station using 2D keypoints. Proc. of the ISPRS Annals of the Photogrammetry, Remote Sensing and Spatial Information Sciences, Enschede, The Netherlands, 10–14.

Medić, T.; Holst, C.; Janßen, J.; Kuhlmann, H. (2019b): Empirical Stochastic Model of Detected Target Centroids: Influence on Registration and Calibration of Terrestrial Laser Scanners. J. Appl. Geodesy 13(201)3, 179–197.

Medić, T.; Kuhlmann, H.; Holst, C. (2019c): Sensitivity Analysis and Minimal Measurement Geometry for the Target-Based Calibration of High-End Panoramic Terrestrial Laser Scanners. Remote Sensing 11(2019)13, 1519.

Medić, T.; Kuhlmann, H.; Holst, C. (2020): Designing and Evaluating a User-Oriented Calibration Field for the Target-Based Self-Calibration of Panoramic Terrestrial Laser Scanners. Remote Sensing 12(2020)1, 15

Mukupa, W.; Roberts, G. W.; Hancock, C. M.; Al-Manasir, K. (2017): A Review of the Use of Terrestrial Laser Scanning Application for Change Detection and Deformation Monitoring of Structures. Survey Review 49(2017)353, 99–116.

Muralikrishnan, B.; Ferrucci, M.; Sawyer, D.; Gerner, G.; Lee, V.; Blackburn, C.; Phillips, S.; Petrov, P.; Yakovlev, Y.; Astrelin, A.; Milligan, S. (2015a): Volumetric Performance Evaluation of a Laser Scanner Based on Geometric Error Model. Precision Engineering 40, 139–150.

Muralikrishnan, B.; Shilling, M.; Rachakonda, P.; Ren, W.; Lee, V.; Sawyer, D. (2015b): Toward the Development of a Documentary Standard for Derived-Point to Derived-Point Distance Performance Evaluation of Spherical Coordinate 3D Imaging Systems. Journal of Manufacturing Systems 37, 550–557.

Muralikrishnan, B.; Rachakonda, P.; Shilling, M.; Lee, V.; Blackburn, C.; Sawyer, D.; Cheok, G.; Cournoyer, L. (2016): Report on the May 2016 ASTM E57.02 Instrument Runoff at NIST, Part 1 – Background Information and Key Findings.

Neitzel, F. (2007): Investigation of Axes Errors of Terrestrial Laser Scanners. Proceedings of the 5th International Symposium Turkisch-German Joint Geodetic Days, Berlin.

Parian, J. A.; Gruen, A. (2010): Sensor Modeling, Self-Calibration and Accuracy Testing of Panoramic Cameras and Laser Scanners. ISPRS J. Photogramm. Remote Sens. 65(2010)1, 60–76.

Reshetyuk, Y. (2010): A Unified Approach to Self-Calibration of Terrestrial Laser Scanners. ISPRS J. Photogramm. Remote Sens. 65(2010)5, 445–456.

Schofield, W.; Breach, M. (2007): Engineering Surveying. 6th ed. Oxford: Elsevier.

Soudarissanane, S. (2016): The Geometry of Terrestrial Laser Scanning; Identification of Errors, Modeling and Mitigation of Scanning Geometry. PhD Thesis, TU Delft.

Vosselman, G.; Maas, H. G. (2010): Airborne and Terrestrial Laser Scanning. CRC press.

Walsh, G. (2015): Leica ScanStation White Paper, HDR for Leica ScanStation P-Series. Leica Geosystems AG.

M. Sc. Tomislav Medić

RHEINISCHE FRIEDRICH-WILHELMS-UNIVERSITÄT BONN, INSTITUT FÜR GEODÄSIE UND GEOINFORMATION

Nußallee 17 | 53115, Bonn
t.medic@igg.uni-bonn.de

Dr.-Ing. Christoph Holst

RHEINISCHE FRIEDRICH-WILHELMS-UNIVERSITÄT BONN, INSTITUT FÜR GEODÄSIE UND GEOINFORMATION

Nußallee 17 | 53115, Bonn
c.holst@igg.uni-bonn.de

Prof. Dr.-Ing. Heiner Kuhlmann

RHEINISCHE FRIEDRICH-WILHELMS-UNIVERSITÄT BONN, INSTITUT FÜR GEODÄSIE UND GEOINFORMATION

Nußallee 17 | 53115, Bonn
heiner.kuhlmann@uni-bonn.de